

Rheological Studies on the Phase Dissolution in a Block Copolymer

RUI XIE,¹ BINGXIN YANG,¹ BINGZHENG JIANG,¹ QIZHONG ZHANG,² YUANZE XU²

¹ Changchun Institute of Applied Chemistry, Chinese Academy of Sciences, Changchun 130022, People's Republic of China

² Beijing Institute of Chemistry, Chinese Academy of Sciences, Beijing 100080, People's Republic of China

Received December 29, 1995; accepted June 25, 1996

ABSTRACT: The microphase transition in a styrene–butadiene–styrene triblock copolymer was studied by rheometric mechanical spectroscopy. A high-temperature-melt rheological transition from the highly elastic, nonlinear viscous behavior typical of a multiphase structure to linear viscous behavior with insignificant elasticity typical of a single-phase structure was observed. The transition temperature is determined according to the discontinuity of the rheological properties across the transition region, which agrees well with the results obtained from the small angle X-ray scattering data and the expectation of the random phase approximation theory. Maybe for the first time, microphase dissolution was investigated rheologically. The storage modulus (G') and the loss modulus (G'') increase with time during the process. An entanglement fluctuation model based on the segmental density fluctuations is presented to explain the rheological behavior in this dissolution process. © 1997 John Wiley & Sons, Inc. *J Appl Polym Sci* **63**: 1155–1164, 1997

INTRODUCTION

Over the past several decades, researchers have reported extensively on the viscoelastic properties of block copolymers. Yet, with a few exceptions, these investigations have dealt exclusively with microphase-separated systems centered around morphology or morphology–property relationships. As a result, the rheological properties of block copolymers near the transition temperatures (T_r) are not well understood and little attention has been paid to the structures of block copolymers at high processing temperatures ($T > T_r$). When the processing temperatures are higher than the transition temperature, it takes time for the block copolymers to finish the transition from

order to disorder state. Unfortunately, this process remains almost unexplored rheologically.

According to Leibler,¹ the critical point in a symmetric diblock copolymer phase diagram occurs at $(\chi N)_c = 10.5$, where N is the degree of polymerization and χ is the interaction parameter. This prediction is based upon an upper critical temperature, often referred to as an upper critical solution temperature for which $\chi > 0$. There may be two ways to make the block copolymers go through the order–disorder transition: vary the polymerization N while keeping the temperature constant so as to bring χN close to the phase boundary; or keep N constant while varying the temperature ($\chi \sim T^{-1}$) to obtain the same effect. In practice, it is more convenient to vary the temperature of the block copolymer, thus providing the means of probing the sample properties and structures through the transition.^{2–8} Recently, the effect of composition fluctuations on the micro-

Correspondence to: R. Xie.

© 1997 John Wiley & Sons, Inc. CCC 0021-8995/97/091155-10

phase separation transition in diblock copolymers has been investigated by Fredrickson and colleagues.^{9,10} The fluctuations are found to be significant for the molecular weight usually encountered; the corrections for that bring the weak segregation theory into better agreement with both experimental and the strong segregation theories.

Small-angle X-ray scattering (SAXS) and small-angle neutron scattering are convenient techniques for probing the sample structures through the transition. Leibler¹ has calculated the correlation function $S(q)$, which characterizes the homogeneous melt state in diblock copolymers:

$$S(q) = N/(F(x) - 2N\chi) \quad (1)$$

where the scattering wave vector $q = 4\pi\lambda^{-1}\sin(\theta/2)$, and x is defined by $x = q^2Na^2/6$, where a is the statistical segment length for blocks A and B (assumed to be identical). $F(x)$ is a combination of Debye functions:

$$F(x) = g_1(1, x)/\{g_1(f_1, x)g_1(1 - f_1, x) - (1/4)[g_1(1, x) - g_1(f_1, x) - g_1(1 - f_1, x)]^2\} \quad (2)$$

where $g(f, x) = (2/x^2)[fx + \exp(-fx) - 1]$. As $2\chi N$ approaches $F(q)$, $S(q)$ diverges. For the critical composition ($\phi = 0.5$), this increment in $S(q)$ corresponds to the development of composition fluctuations of periodicity, $D = \pi R$, with R the overall radius of gyration of the block copolymers. The point of divergence, $\chi N = (\chi N)_s$, defines the stability limit, which establishes the spinodal curve over all compositions. It implies that the scattering intensity reaches its maximum at the spinodal points. Thus, the spinodal points can be determined experimentally.³⁻⁸

Kinetic studies of the microphase dissolution in block copolymers were performed by Hashimoto and associates,^{4,5} who studied the styrene-butadiene diblock copolymer (SB) in the solvent n -tetradecane by time-resolved SAXS. Their results suggest that the segmental density fluctuations decay exponentially with time on a time scale much larger than τ , the retardation time required to achieve the experimental temperature by the T-jump method:

$$\Delta\rho_k(q, t) = \rho_k(q, 0)(\exp(-R(q)t) - 1) \quad (3)$$

$$R(q) = q^2D_c(\chi_s - \chi)/\chi_s = q^2D_{\text{eff}} \quad (4)$$

where $\rho_k(q, t)$ and $\rho_k(q, 0)$ are the segmental density fluctuations at time t and time 0 for polymer k , respectively, χ_s is the χ value at the spinodal point, and D_{eff} is the effective diffusivity.

Transitions in block copolymers have also been studied rheologically.¹¹⁻²⁰ Chung and Lin¹¹ and Gouinlock and Gale¹² have examined the dynamic mechanical properties of a styrene-butadiene-styrene (SBS) triblock copolymer at elevated temperatures and have reported similar results. Both groups related the discontinuity of dynamic elastic modulus and dynamic viscosity at low frequency as a function of temperature to the block copolymer microphase separation transition. Recently, extensive rheological investigations on the order-disorder transition in both the block copolymer and block copolymer/homopolymer blends have been conducted by Bates and associates¹³⁻¹⁶ and Han and colleagues.¹⁷⁻²⁰ They were successful in determining the order-disorder transition temperature as well as modification of Leibler's results for fluctuation effects.^{14,17}

The present text will first focus on the rheological behavior near the transition temperature; then the rheological behavior during microphase dissolution ($T > T_c$) will be carefully discussed. An entanglement fluctuation model based on the segmental density fluctuations is presented, which explains qualitatively the rheological behavior during phase dissolution and provides better understanding of the rheological behavior as microphase dissolution proceeds.

EXPERIMENTAL

The SBS triblock copolymer used here is a commercial product of Aldrich Chemical Company, containing 28 wt % of polystyrene. The number-average molecular weight, M_n , is 52,000, and the polydispersity index, M_w/M_n , is 1.36, as determined by membrane osmometry and gel permeation chromatography, respectively.

Dynamic moduli were determined with the Rheometrics Mechanical Spectrometer 605 in an oscillating parallel-plate in the linear viscoelastic region (under strains of 0.3–1%). The frequency was varied from 0.01 to 100 rad/s. Time sweeps were performed at constant temperatures with a constant frequency of 1.5 rad/s. Gaps between the plates was 1 mm for all experiments. The sample was molded at 140°C to form a circular disc with a diameter and thickness of 25 mm and 1.5 mm,

respectively, and was stored and mounted onto the plate.

SAXS measurements were conducted with a Kratky Compact Small Angle System equipped with a stationary-anode copper-target X-ray tube (wavelength 1.54 Å). All SAXS data were recorded with a one-dimensional position detector and allowed to add up over 10^5 in order to reduce statistical errors. The measured intensity was corrected for background scattering and desmeared by the method proposed by Strobl.²¹ A moving-slit device was used to measure the absolute intensity. Samples were molded at 140°C to form strips (ca. 25 mm × 5 mm × 2.5 mm) which were inserted into the sample holder whose temperature could be controlled from 25°C to 300°C within $\pm 1^\circ\text{C}$.

Dynamic mechanical behavior of SBS was measured with a Rheovibron Dynamic Viscoelastometer (DDV-II-EA, Japan). The block copolymer was molded at 140°C to form films of 0.3 mm thickness; the films were then cut into strips 50 mm long and 4 mm wide. Annealing was performed at 165°C in air for 1 h for strips sandwiched by two aluminum pallets.

DESCRIPTION OF THE MODEL

Problems in block copolymers are generally considered as polymer blends for simplicity. In a phase-separated polymer mixture, the physics is similar to that in block copolymers apart from the joints between segments. If one considers a two-phase system composed of phases *A* and *B* with ϕ_A and ϕ_B the volume fractions of *A* and *B* phases, respectively, assuming that the blend is of sharp interface, then there are no *A* molecules in the *B* phase and vice versa. Thus, $\rho_{0A} = \rho_{0B} = 1$, where ρ_{0A} and ρ_{0B} are the reduced segment densities of *A* and *B* phases, respectively; and $\rho_{0K} = \rho_K(x)/\rho_{PK}$ ($K = A, B$), with $\rho_K(x)$ the segment density of *K* phase at x , and ρ_{PK} the segment density of pure polymer *K*. As phase dissolution proceeds, there are segment density fluctuations $\Delta\rho_A$ and $\Delta\rho_B$ in both *A* and *B* phases. The numbers of *A* and *B* molecules in *A* phase are $(\rho_{0A} - \Delta\rho_A)\phi_A$ and $\Delta\rho_B\phi_B$, respectively, and those in *B* phase are $\Delta\rho_A\phi_A$ and $(\rho_{0B} - \Delta\rho_B)\phi_B$, respectively, while the total number of molecules in the system remains constant during the fluctuations. Therefore, one may consider that *A* phase as a miscible blend which is rich in *A* molecules and poor in *B* molecules, and similar consideration can be applied to

the *B* phase. Hence, a simple analysis of entanglement after considering pairwise interactions in a blend represented by Wu²² can be applied to the present case. This consideration leads to a number of entanglements along one chain:

$$\begin{aligned} n_e &= P_{AA}(N_{0A}/N)^2 + P_{BB}(N_{0B}/N)^2 \\ &+ 2P_{AA}(\Delta\rho_A\phi_A/N)^2 + 2P_{BB}(\Delta\rho_B\phi_B/N)^2 \\ &- 4P_{AB}(\Delta\rho_A\phi_A/N)(\Delta\rho_B\phi_B/N) \\ &- 2(P_{AA}\Delta\rho_A\rho_{0A}\phi_A^2 + P_{BB}\Delta\rho_B\rho_{0B}\phi_B^2)/N^2 \\ &- P_{AB}(\Delta\rho_B\rho_{0A} + \Delta\rho_A\rho_{0B})\phi_A\phi_B/N^2 \\ &= n_{e0} + \Delta n_e \quad (5) \end{aligned}$$

and

$$n_{e0} = P_{AA}(N_{0A}/N)^2 + P_{22}(N_{0B}/N)^2 \quad (6)$$

$$\begin{aligned} \Delta n_e &= 2[P_{AA}(\Delta\rho_A\phi_A)^2 + P_{BB}(\Delta\rho_B\phi_B)^2 \\ &- 2P_{AB}(\Delta\rho_A\Delta\rho_B\phi_A\phi_B)]/N^2 \\ &- 2(P_{AA}\Delta\rho_A\rho_{0A}\phi_A^2 + P_{BB}\Delta\rho_B\rho_{0B}\phi_B^2) \\ &- P_{AB}(\Delta\rho_B\rho_{0A} + \Delta\rho_A\rho_{0B})\phi_A\phi_B/N^2 \quad (7) \end{aligned}$$

$$N = N_{0A} + N_{0B} \quad (8)$$

where N_{0A} and N_{0B} are the total number of chains of polymer *A* and polymer *B* in the blend, respectively; P_{ij} is the contact probability between two polymer chains ($i, j = 1, 2$); n_{e0} represents the number of entanglements in the phase-separated blend; and Δn_e is the contribution from the concentration fluctuations as the phase dissolution initiates.

It is reasonable to assume an incompressible system with no volume change upon dissolution. Thus, $\Delta\rho_B = -(\rho_{PB}/\rho_{PA})(M_A/M_B)(\phi_A/\phi_B)\Delta\rho_A$, where M_A and M_B are the segmental weights of polymers *A* and *B*, respectively. If $\beta = (\rho_{PB}/\rho_{PA})(M_A/M_B)(\phi_A/\phi_B)$, considering that $\phi_A + \phi_B = 1$, and $\rho_{0A} = \rho_{0B} = 1$, then

$$\Delta n_e = \gamma\Delta\rho_A^2 + 2\lambda\Delta\rho_A \quad (9)$$

where $\gamma = 2(P_{AA}\phi_A^2 + P_{BB}\beta^2\phi_B^2 - 2P_{AB}\beta\phi_A\phi_B)$, $\lambda = -(P_{AA}\rho_{0A}\phi_A^2 + P_{BB}\beta\rho_{0B}\phi_B^2 - P_{AB}(\rho_{0A}\beta + \rho_{0B})\phi_A\phi_B)$. Obviously, γ and λ are the character-

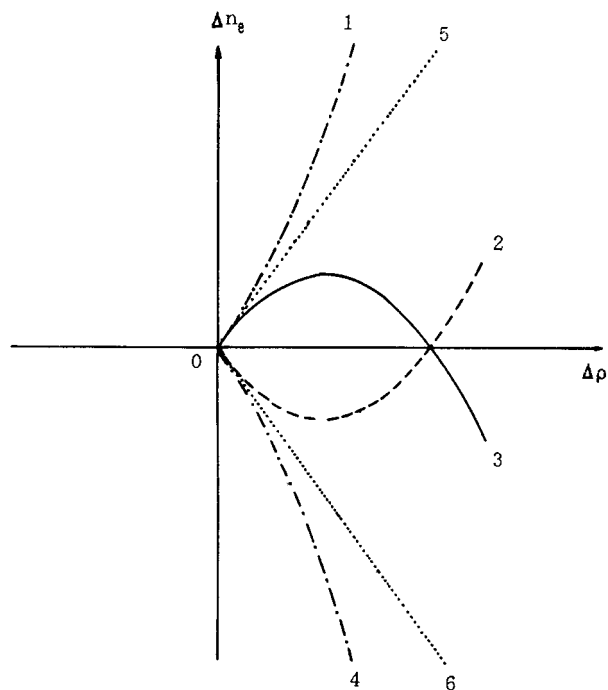


Figure 1 Variation of Δn_e with segmental density fluctuations $\Delta \rho_k$ during phase dissolution: curve 1 ($A > 0, B > 0$); curve 2 ($A > 0, B < 0$); curve 3 ($A < 0, B > 0$); curve 4 ($A < 0, B < 0$); curve 5 ($A = 0, B > 0$); curve 6 ($A = 0, B < 0$).

istics of a given system. As shown in Figure 1, Δn_e changes with $\Delta \rho_A$ in six ways:

1. $\gamma > 0, \lambda > 0$. Δn_e increases with $\Delta \rho_A$ as phase dissolution proceeds, as indicated by curve 1.
2. $\gamma > 0, \lambda < 0$. Δn_e varies with $\Delta \rho_A$ according to curve 2. Δn_e first decreases, then increases with $\Delta \rho$.
3. $\gamma < 0, \lambda > 0$. Δn_e varies with $\Delta \rho_A$ according to curve 3. Δn_e first increases, then decreases with $\Delta \rho_A$.
4. $A < 0, B < 0$. Δn_e varies with $\Delta \rho_A$ according to curve 4. Δn_e decreases with $\Delta \rho_A$.
5. $A = 0, B > 0$. Δn_e varies with $\Delta \rho_A$ according to curve 5. Δn_e increases linearly with $\Delta \rho_A$.
6. $A = 0, B < 0$. Δn_e varies with $\Delta \rho_A$ according to curve 6. Δn_e decreases linearly with $\Delta \rho_A$.

According to Wu,²² $P_{AA} = \rho_{PA}/M_{eA}$, $P_{PB} = \rho_{PB}/M_{eB}$, and $P_{AB} = (\rho_{PA}\rho_{PB})^{1/2}/M_{eAB}$. The M_{eA} and M_{eB} are the entanglement molecular weights of pure components A and B, respectively, and M_{eAB}

is that of a hypothetical pure component of density $(\rho_{PA}\rho_{PB})^{1/2}$ having the entanglement probability as that between the two dissimilar chains in the blend. If $M_{eAB} < (M_{eA}M_{eB})^{1/2}$, then $\gamma > 0$. It implies that M_{eAB} is a very important parameter which determines the behavior of entanglement fluctuations during phase dissolution.

Since a melt of polymers consists of long chains, the entanglements between chains make the polymer behave like a "rubber" network for times $t < \tau_t$, where τ_t is the terminal relaxation time. We may visualize the polymer chain as a succession of units or "blobs" of size ξ . Thus the melt is essentially a closely packed system of blobs and the network made of entanglements of polymers is essentially constructed by the interpenetrating blobs. Considering this, the elastic modulus is²³

$$E \approx T/(\xi^3 n_v) \quad (10)$$

where T is the absolute temperature; ξ is the size of the blob; and n_v represents the average interval between entanglement points along one chain. It can be also written as

$$E \approx T n_e / \xi^3 \quad (11)$$

From eq. (10), one can see that the elastic modulus is proportional to n_e since the size of blobs remains unchanged at constant temperatures. The viscosity, η , can be expressed as

$$\eta \approx \tau_t E \quad (12)$$

For a polymer with definite chain length, τ_t is a constant. Therefore, the viscosity is also proportional to n_e .

Combining eqs. (5), (11), and (12), the effects of entanglement fluctuation on the elastic modulus E and viscosity η during phase dissolution are clear. Although the model is based on the blends of homopolymers, because segmental density fluctuations exist in both homopolymer blends and block copolymers, the model still applies to block copolymers; however the segmental density fluctuations are different between the two systems.^{4-5,24} Thus the entanglement fluctuation induced by segmental density fluctuations should also be different between the two systems.²⁵ However, this has no effect on the applicabilities of the model.

The values of n_e calculated according to eqs. (4) and (5) during microphase dissolution are shown

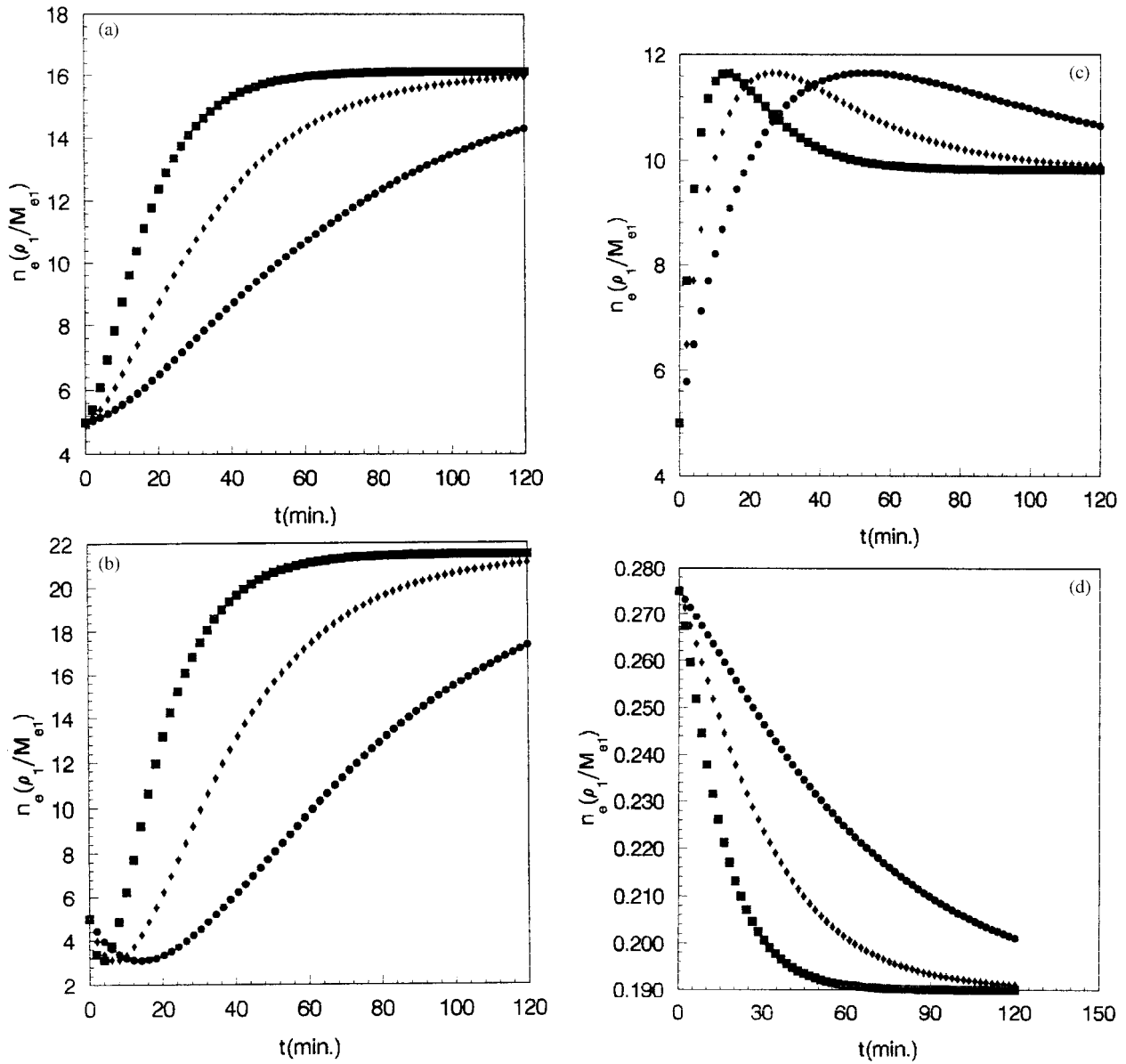


Figure 2 Variation of n_e with time t during phase dissolution at different values of R : $R = 0.02$ (\bullet), $R = 0.04$ (\blacklozenge), $R = 0.08$ (\blacksquare). (a) $M_{eA} = 9M_{eB} = 18M_{eAB}$, (b) $M_{eA} = 9M_{eB} = 3M_{eAB}$, $M_{eA} = 9M_{eB} = 30M_{eAB}$, and $M_{eA} = 10M_{eB} = 2.7M_{eAB}$ for Figure 2(a), (b), (c), and (d), respectively, which correspond to $\gamma > 0$, $\lambda > 0$; $\gamma > 0$, $\lambda < 0$; $\gamma < 0$, $\lambda > 0$; and $\gamma < 0$, $\lambda < 0$. The other parameters used in the calculation were based on the characteristics of the SBS block copolymer and set to be $\phi_A = 0.26$, $\phi_B = 0.74$, $\rho_{0A} = \rho_{0B} = 1$, $\rho_A = \rho_B = 1$, and $M_A/M_B = 1.925$. According to Hashimoto and associates,⁵ the amplification factor $R(q)$ in eq. (4) is of the order

in Figure 2. In order to make the calculation simple, we assumed that $M_{eA} = 9M_{eB} = 18M_{eAB}$, $M_{eA} = 9M_{eB} = 3M_{eAB}$, $M_{eA} = 9M_{eB} = 30M_{eAB}$, and $M_{eA} = 10M_{eB} = 2.7M_{eAB}$ for Figure 2(a), (b), (c), and (d), respectively, which correspond to $\gamma > 0$, $\lambda > 0$; $\gamma > 0$, $\lambda < 0$; $\gamma < 0$, $\lambda > 0$; and $\gamma < 0$, $\lambda < 0$. The other parameters used in the calculation were based on the characteristics of the SBS block copolymer and set to be $\phi_A = 0.26$, $\phi_B = 0.74$, $\rho_{0A} = \rho_{0B} = 1$, $\rho_A = \rho_B = 1$, and $M_A/M_B = 1.925$. According to Hashimoto and associates,⁵ the amplification factor $R(q)$ in eq. (4) is of the order

$10^{-2}/\text{min}$, thus, $R(q)$ was set to be 0.02, 0.04, and 0.08 in the calculation for different curves in Figure 2. As shown in Figure 2(a), n_e increases with time in the first tens of minutes and approaches its plateau value gradually. In Figure 2(b), n_e decreases in the first 10 min, then increase rapidly before reaching its plateau value. In Figure 2(c), n_e increases rapidly in the first tens of minutes, then decreases slowly until reaching its plateau value. In Figure 2(d), n_e decreases with time and then approaches its plateau value. The higher $R(q)$ is, the more rapidly n_e changes, implying

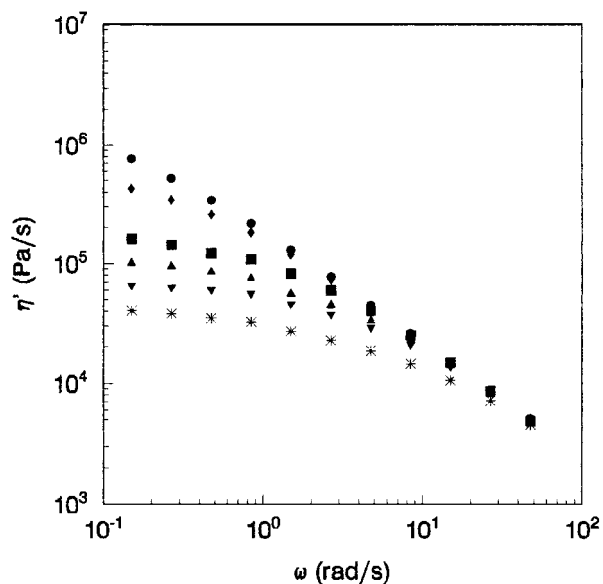


Figure 3 Dynamic viscosity as a function of angular frequency for SBS copolymer. Temperature ($^{\circ}\text{C}$): 99 (\bullet), 107 (\blacklozenge), 117 (\blacksquare), 123 (\blacktriangle), 135 (\blacktriangledown), 144 ($+$), 158 (\times).

that the temperature at which the dissolution occurs has a great effect on the behavior of n_e .

For microphase dissolution in block copolymers, the size of the blobs should remain constant at a constant temperature. From eqs. (10) and (11), one can expect that the elastic modulus and the elastic viscosity will vary with time in the same ways as n_e during microphase dissolutions. In the next section, rheological behavior of block copolymers during microphase dissolution is discussed in the context of the presented model.

RESULTS AND DISCUSSION

Order-Disorder Transition in Block Copolymers

The dynamic viscosity (η') and the storage modulus (G') measured at seven temperatures are compiled as a function of angular frequency (ω) in Figures 3 and 4, respectively. Referring to Figure 3, $\eta'(\omega)$ is much more independent of ω for low-angular frequencies at temperatures above 107°C than that below 107°C . The high elasticity exhibited by the sample above 107°C is evident in Figure 4. The storage modulus for low-angular frequencies decreases conspicuously between 99°C and 117°C , as shown in Figure 4. Figure 5 shows that the dynamic modulus of the sample undergoes a pronounced transition over a temper-

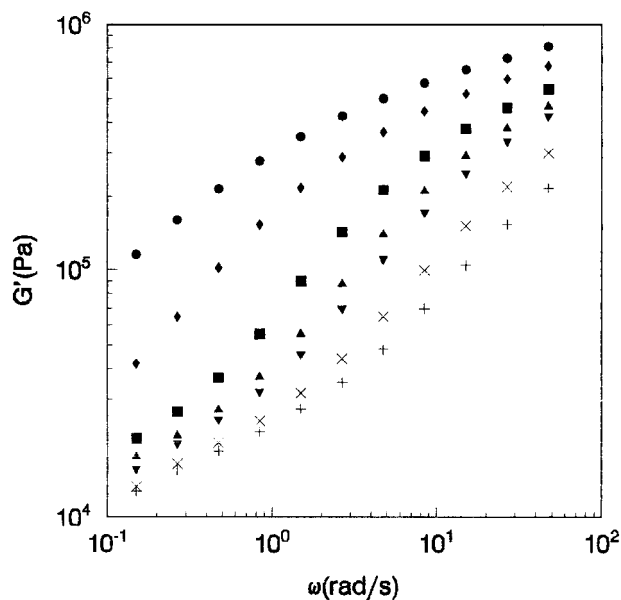


Figure 4 Storage modulus as a function of angular frequency for SBS copolymer. Symbols are the same as in Figure 3.

ature region of about $99\text{--}117^{\circ}\text{C}$. The transition is clearly seen at low values of ω . From the results shown in Figures 3, 4, and 5, one can conclude

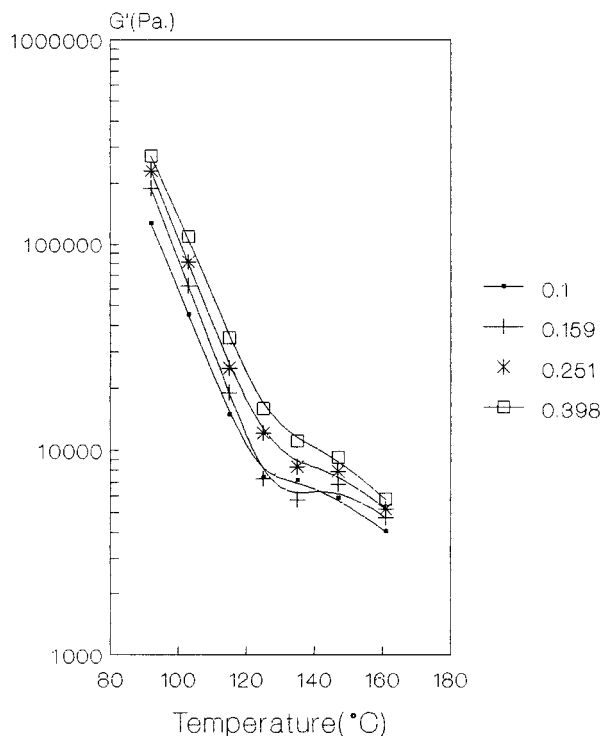


Figure 5 Dynamic modulus at a constant angular frequency as a function of temperature for SBS copolymer.

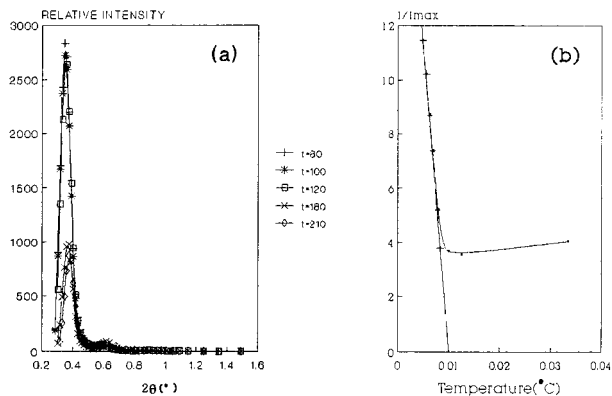


Figure 6 Determination of transition temperatures of SBS from SAXS data. (a) SAXS curves for SBS at different temperatures; (b) reciprocal of the intensity I_{max} against the reciprocal of the temperature. A linear extrapolation of $1/I_{max}$ at high temperatures to zero gives the spinodal temperature while the first deviation of the observed intensity from the straight line gives the order-disorder transition temperature.

that in the neighborhood of 107°C, the rheological behavior undergoes a pronounced transition.

To obtain a better understanding of the rheological transition, SAXS experiments were performed. The order-disorder transition temperature was determined to be the temperature at which the intensity of the first-order peak is hardly discernible. According to eq. (1), the reciprocal of the scattered intensity ($1/I$) should be a linear function of the interaction parameter χ . If χ is proportional to the reciprocal of the absolute temperature $1/T$, the plot of $1/I$ versus $1/T$ should give a straight line in the disordered state. The order-disorder temperature can thus be determined as the temperature at which the linear relationship between $1/I$ and $1/T$ starts to deviate. The order-disorder transition and the spinodal decomposition temperatures of the sample determined in this way are 115°C and 100°C, respectively, as shown in Figure 6. The result is relatively close to that obtained rheologically. Therefore, the structural transition which accompanies with the rheological transition is the same as the structural transition observed by SAXS.

From eqs. (1) and (2), the spinodal decomposition point $(\chi N)_s$ can be determined theoretically. Using a method similar to that of Hashimoto and colleagues,^{26,27} $(\chi N)_s$ was found to be 32.3 for the present sample, which was very close to the published data of Mayes and Olvera de la Cruz.²⁸ According to Owens and coworkers,²⁹ the interaction

parameter χ_{SB} between styrene and butadiene obeys

$$\chi(t) = 25/T - 0.021 \quad (13)$$

where T is the absolute temperature. Based on the given molecular weight and composition of the copolymer, we deduced $N \approx 1130$. Thus, χ_s , the value of χ at which spinodal decomposition occurs, is found to be 0.0286. From eq. (13), the spinodal decomposition temperature can be calculated to be about 504 K. This value is much larger than that determined experimentally (ca. 373 K). Similar divergence between the theoretical and experimental results were also reported by Zin and Roe,³⁰ who found that the theoretical value of the spinodal decomposition temperature was about 1.5 times that determined by SAXS. There may be two factors that give rise to the difference. First, the random phase approximation theory of block copolymers presented by Leibler¹ is based on nearly continuous transitions and not applicable if transitions are first-order, which is the case with triblock and asymmetric diblock copolymers.

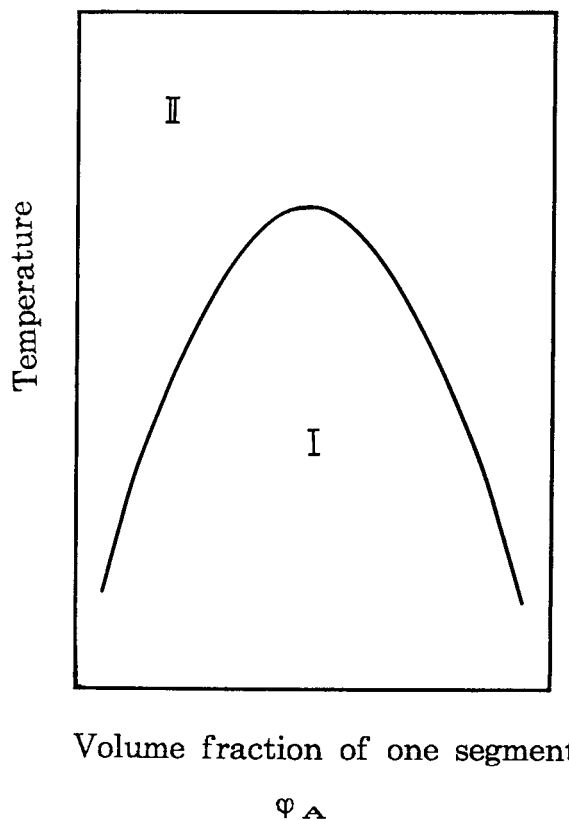


Figure 7 Phase diagram of block copolymers: (I) ordered, (II) disorder.

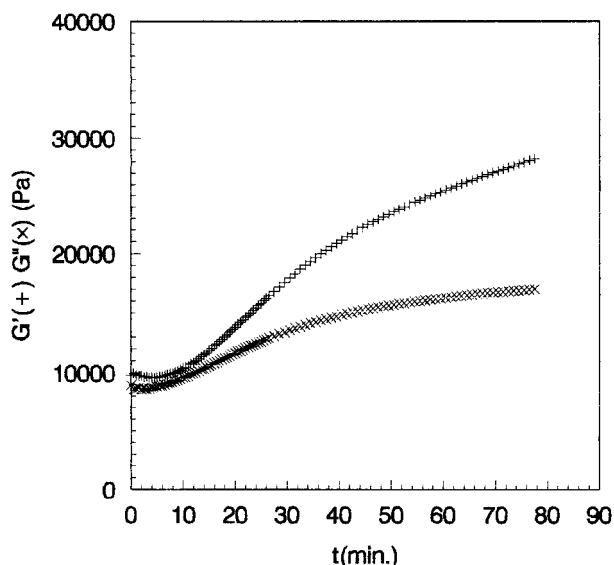


Figure 8 Variation of G' and G'' with time t during microphase dissolution at 166°C : G' (+), G'' (x).

Recent Monte Carlo simulation studies on both symmetric and asymmetric diblock copolymers show that the theory is not valid to some extent.^{31,32} Second, the relatively high polydispersity of the present copolymer may have great effects on its transition behavior. Under these considerations, we would rather believe the experimental result than the calculated one.

Microphase Dissolution in Block Copolymers

Figure 7 is a typical phase diagram for block copolymers. As the sample goes from the phase-separated to the homogeneous region, the multiphase structure gradually disappears due to the miscibility between segments. This process is called "phase dissolution." Figure 8 shows the time sweeps of G' and G'' during microphase dissolution at 166°C . Both G' and G'' increase with time after the initiation of the microphase dissolution. Both increase more rapidly in the first 30 min as compared with the increase after the first 30 min. The variations of G' and G'' with time imply that physical and/or chemical reactions occur in the sample. Since the time-sweep experiments were carried out at temperatures much higher than T_c , microdomain morphology in the triblock copolymer changed with time, which would contribute to the increases in G' and G'' . On the other hand, the oxide or degradation of the polymer may also bring about the increases in G' and G'' , especially considering the experimental temperature and

the polybutadiene (PB) segments in the copolymer. In Figure 9, we present the dynamic mechanical behavior of SBS before and after annealing at 165°C in air for 1 h. The annealed sample shows a lower glass transition temperature (T_g) of PB and a lower elastic modulus in the whole experimental temperature, but an almost identical T_g of polystyrene as compared to the unannealed one. The results suggest that the oxide or degradation of PB does not lead to the increases in G' and G'' . Since the annealing condition of the sample for the dynamic mechanical measurement is very close to the thermohistory of SBS after time sweeps, we deduce that the increases in G' and G'' are due to phase dissolution. Such a consideration reminds us of the physical entanglements between polymer chains.

It is interesting to compare the results shown in Figure 8 with those shown in Figure 2(b). The rheological behavior is quite similar to the variations in n_e as predicted by the represented model. Since the elastic modulus E and the viscosity η are proportional to n_e , the behavior of n_e described in Figure 2 is essentially a reflection of the rheological behavior of E and η . Because of this, we would like to claim that the entanglement fluctu-

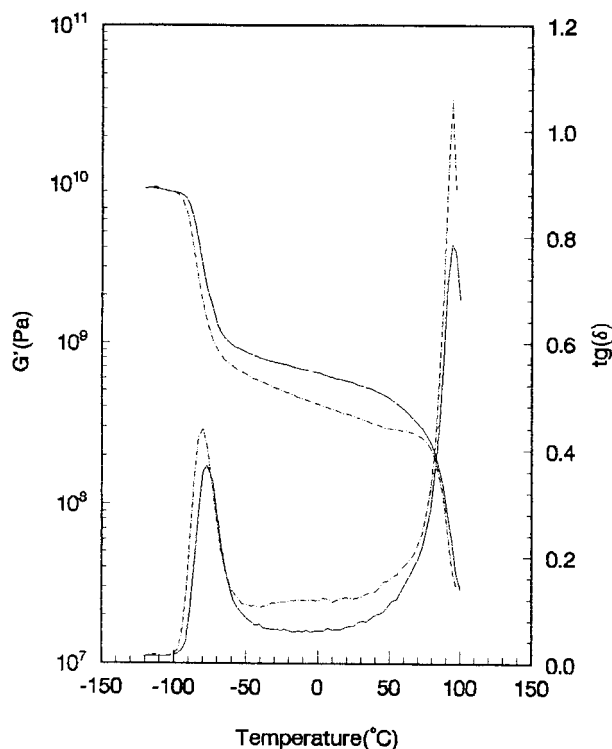


Figure 9 Dynamic mechanical behavior of SBS before (—) and after (---) annealing at 165°C for 1 h.

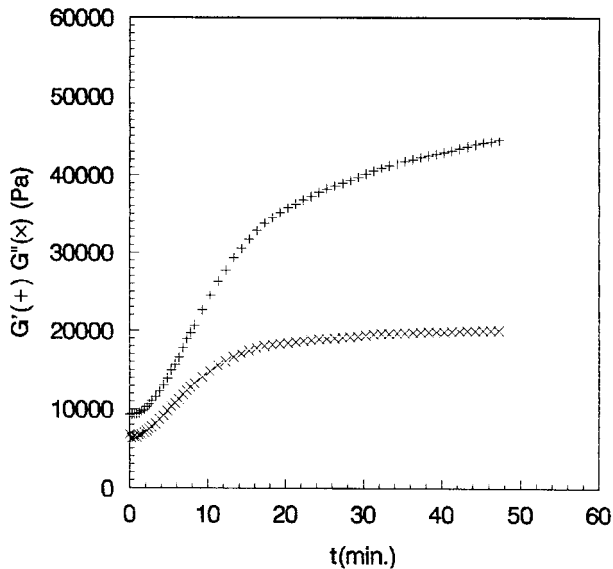


Figure 10 Variation of G' and G'' with time t during microphase dissolution at 177°C: G' (+), G'' (×).

ation induced by the segment density fluctuations results in the variations of rheological properties during phase dissolution.

One may argue that E and η in eqs. (11) and (12) are not the G' and G'' shown in Figure 8. However, under some approximations there are still relationships between the measured G' , G'' , and E . For the Newtonian fluid, $E \approx 3G$, where G is the steady shear modulus, can be related to the dynamic modulus G' and G'' in the frame of the Maxwell model by

$$E = 3G = (1 + \omega^2\tau_l^2)G' / (\omega^2\tau_l^2) \\ = (1 + \omega^2\tau_l^2)G'' / (\omega\tau_l) \quad (14)$$

where ω and τ_l are the frequency and terminal time, respectively. For the non-Newtonian fluid, the relationship between the elastic modulus and the shear modulus is still an open question. As the ω used in the experiment is a constant and relatively low, and the dissolution process is essentially a transition from the non-Newtonian to the Newtonian fluid, although the block copolymer investigated here is a non-Newtonian fluid we suppose that it is very close to the Newtonian fluid. Under this approximation, the proportional relationships between E and G' , $G''(\eta')$ can be expected. Thus, the behavior of n_e during phase dissolution described in Figure 2 remains an approximate description of G' and $G''(\eta')$.

Figure 10 shows time sweeps of G' and G'' dur-

ing microphase dissolution at 177°C. In the first 15 min, G' and G'' almost reach their plateau values, and then increase with time very slowly. Both increase more rapidly in the first 10 min than they do at 166°C. This is reasonable from the model. As the dissolution temperatures increase, the effective diffusivity D_{eff} increases.⁵ According to eq. (4), the amplification factor $R(q)$ increases. Thus, the larger $R(q)$ is, the more rapidly n_e increases, as shown in Figure 2. Therefore, the model can describe the rheological behavior of the block copolymers at different dissolution temperatures.

CONCLUSION

We have studied rheologically the order–disorder transition and the microphase dissolution in a triblock copolymer. It is evident that the rheological transition in block copolymers arises from the order–disorder transition, as shown by the SAXS and rheological results. The transition behavior has also been discussed in the frame of RPA theory proposed by Leibler,¹ and the experimental results have been found to agree with the theoretical results as considering the shortcoming of the theory itself and the polydispersity of the sample. The rheological behavior during microphase dissolution is important and worth further investigation. The entanglement fluctuation model described here suggests that the rheological behavior during microphase dissolution is essentially the result of entanglement fluctuations originating from the segmental density fluctuations.

However, there are still problems unsolved. First, at present there are no experimental data which equate the value of $R(q)$ during microphase dissolution in bulk state. $R(q)$ determined in scattering experiments is a function of q , so the notation may be different from the one used here. We anticipate that a corresponding amplification factor $R(\omega)$, which describes the segmental density fluctuations in rheological experiments, should exist and probably relates to $R(q)$. Second, the relationship between E and G' (G'') for the non-Newtonian fluid is still unclear. Since it is difficult to perform steady elongation experiments (measure E and η) for polymer fluids, the relationship between E and G' (G'') is yet to be established. Otherwise, new techniques should be innovated in order to measure E and η directly. Finally, the size of blob, to our knowledge, has not appeared in publications. We have not found any techniques which are suitable for determining the size of the

blob. However, if the first two problems are resolved, the blob size can be measured experimentally.

We feel that the time-sweep technique used here is a powerful method of studying the dynamics of phase separation and phase dissolution rheologically.²⁵ It also provides a method of detecting the phase structure near T_r . Recently, multiple ordered phases have been detected near T_r by Almdal and colleagues.¹⁵ Thus, time sweeps at different temperatures near T_r will give the information of order–order or order–disorder transitions, which provides critical proofs for the mean-field theory¹ or the fluctuation-corrected mean-field theory.⁹ Detailed investigations are in process.

The financial support of this work is from the National Basic Research Project—Macromolecular Condensed State.

REFERENCES

1. L. Leibler, *Macromolecules*, **13**, 1602 (1980).
2. F. S. Bates and M. A. Hartney, *Macromolecules*, **18**, 2487 (1985).
3. T. Hashimoto, M. Shibayama, H. Kawai, H. Watanabe, and T. Kotaka, *Macromolecules*, **16**, 361 (1983).
4. T. Hashimoto, K. Kowsaka, M. Shibayama, and H. Kawai, *Macromolecules*, **19**, 750 (1986).
5. T. Hashimoto, K. Kowsaka, M. Shibayama, and H. Kawai, *Macromolecules*, **19**, 754 (1986).
6. R. J. Roe, M. Fishkis, and J. C. Chang, *Macromolecules*, **14**, 1091 (1981).
7. W. C. Zin and R. J. Roe, *Macromolecules*, **17**, 183 (1984).
8. S. Nojima and R. J. Roe, *Macromolecules*, **20**, 1866 (1987).
9. G. H. Fredrickson and E. Helfand, *J. Chem. Phys.*, **87**, 697 (1987).
10. G. H. Fredrickson and R. G. Larson, *J. Chem. Phys.*, **86**, 1553 (1987).
11. C. I. Chung and M. I. Lin, *J. Polym. Sci., Polym. Phys. Ed.*, **16**, 545 (1978).
12. E. V. Gouinlock and J. C. Gale, *Polym. Eng. Sci.*, **17**, 573 (1977).
13. J. H. Rosedale and F. S. Bates, *Macromolecules*, **23**, 2329 (1990).
14. F. S. Bates, J. H. Rosedale, and G. H. Fredrickson, *J. Chem. Phys.*, **92**, 6255 (1990).
15. K. Almdal, K. A. Koppi, F. S. Bates, and K. Mortensen, *Macromolecules*, **25**, 1743 (1992).
16. M. D. Gehlsen, K. Almdal, and F. S. Bates, *Macromolecules*, **25**, 939 (1992).
17. C. D. Han, J. Kim, and J. K. Kim, *Macromolecules*, **22**, 383 (1989).
18. C. D. Han, D. M. Baek, J. Kim, K. Kimishima, and T. Hashimoto, *Macromolecules*, **25**, 3052 (1992).
19. D. M. Baek and C. D. Han, *Macromolecules*, **25**, 3706 (1992).
20. J. Kim and C. D. Han, *J. Polym. Sci., Polym. Phys. Ed.*, **26**, 677 (1988).
21. G. R. Strobl, *Acta Crystallogr. A*, **26**, 367 (1970).
22. S. Wu, *J. Polym. Sci., Polym. Phys. Ed.*, **25**, 2511 (1987).
23. P. G. de Gennes, *Scaling Concepts in Polymer Physics*, Cornell University Press, Ithaca and London, 1979.
24. J. Kumaki and T. Hashimoto, *Macromolecules*, **19**, 763 (1986).
25. R. Xie, H. G. Liang, B. X. Yang, B. Z. Jiang, Q. Zhang, and Y. Xu, *J. Appl. Polym. Sci.*, **50**, 1397 (1993).
26. K. Mori, H. Tanaka, and T. Hashimoto, *Macromolecules*, **20**, 381 (1987).
27. J. K. Kim, K. Kimishima, and T. Hashimoto, *Macromolecules*, **26**, 125 (1993).
28. A. M. Mayes and M. Olvera de la Cruz, *J. Chem. Phys.*, **91**, 7228 (1987).
29. J. N. Owens, I. S. Gancarz, J. T. Koberstein, and T. P. Russell, *Macromolecules*, **22**, 3380 (1989).
30. W. Zin and R. Roe, *Macromolecules*, **17**, 183 (1984).
31. H. Fried and K. Binder, *J. Chem. Phys.*, **94**, 8349 (1991).
32. K. Binder and H. Fried, *Macromolecules*, **26**, 6878 (1993).